International Journal of Applied Engineering Research ISSN 0973-4562 Volume 13, Number 10 (2018) pp. 7692-7700

Structural and optical properties of Nd^{3+}- doped lead borosilicate glasses for broadband laser amplification

M. Reddi Babu[a], A. Mohan Babu[a*], L. Rama Moorthy[a]

[a]*Department of Physics, Chadalawada Ramanamma Engineering College, Tirupati - 517 506, India.*

**Corresponding Author*

Abstract

In the present work, neodymium (Nd^{3+}) doped lead borosilicate glasses (NLBS) were prepared using the various chemical constituents such as PbO, H_3BO_3, SiO_2, Al_2O_3, LiF and Nd_2O_3 by the conventional melt-quenching method. The structural properties of the NLBS glasses were investigated through the X-ray diffraction (XRD), Fourier transform Infrared (FTIR) spectral measurements; whereas the optical properties such as intensity parameters (Ω_λ), radiative transition probabilities (A_R), total transition probability (A_T), radiative lifetime (τ_R) and branching ratios (β_R) have been determined from the UV-VIS-NIR absorption and emission spectra. From the XRD analysis, the amorphous nature of NLBS glasses has been confirmed and the functional groups as well as the co-existence of trigonal BO_3 and tetrahedral BO_4 units are identified from the IR spectra. The experimental and calculated oscillator strengths (f_{exp} & f_{cal}) and the evaluated Judd-Ofelt (JO) intensity parameters (Ω_λ, λ = 2, 4 and 6) were determined from the absorption spectrum and compared with the other Nd^{3+} doped host glasses. From the recorded emission spectra, three NIR bands identified at 903, 1060 and 1334 nm corresponding to the $^4F_{3/2}\rightarrow{}^4I_{9/2}$, $^4F_{3/2}\rightarrow{}^4I_{11/2}$ and $^4F_{3/2}\rightarrow{}^4I_{13/2}$ transitions, respectively for which the effective bandwidths ($\Delta\lambda_P$), radiative transition probabilities (A_R), branching ratios (β_R), and stimulated emission cross-sections (σ_e) were also evaluated. The intensities of emission bands increased with the increase of Nd^{3+} ions concentration upto 1.0 mol% and then decreased at higher concentrations due to the concentration quenching. From the results of these investigations, it is concluded that the Nd^{3+} doped LBS glasses could be useful for various photonic applications in different fields.

Keywords: Lead borosilicate glasses; Structural properties; JO analysis; Intensity parameters; Optical properties

INTRODUCTION

In the modern era, the variety of oxide glasses are incorporated with various rare earths ions (RE^{3+}) have attracted the several researchers and technologists due to their unique properties such as trouble-free casting, good transparency, solubility of rare earth ions and long term stability **[1-9]**. However, due to the increasing demand of the rare earth doped multi-component oxide laser glasses in various applications such as higher order harmonic generation**,** time-resolved laser spectroscopy, plasma generation, laser abalation, fusion drive and in many more areas **[10-14]**; In order to meet the desired specifications, a good host glass is highly essential to improve the quantum efficiency. In the process of searching of various oxide glasses, the host glasses with heavy metallic components like lead oxide, aluminum oxide and silicon dioxide are found to have the ultrafine transparency, high thermal stability, low melting point, infrared transparency, corrosion resistance and also good solubility of rare earth ions **[15, 16]**. In these multi-constituents, the role of lead in the glass network is to reduce the phonon energy of borate (~1400cm^{-1}) and also to increase the mechanical stability by lowering the melting temperature. Hence, in the present study the lead borosilicate glasses (LBS) are chosen as a host matrix to meet the specified applications. Among rare earth ions, the neodymium (Nd^{3+}) ion is identified as one of the most efficient ions for solid state lasers with the emission wavelength at 1060 nm as well as the possibility for lasing action at other wavelengths such as 1800, 1350 and 880 nm which are be useful for broadband laser amplifiers and other photonic applications **[17, 18].** The intensities of Nd^{3+} ion absorption bands have been analyzed using the Judd-Ofelt (JO) analysis **[19, 20]**. The JO analysis leads the evaluation of set of three intensity parameters Ω_2, Ω_4 and Ω_6, which are sensitive to the environment of rare earth ion doped glass matrices. From these intensity Ω_λ, (λ = 2, 4 and 6) parameters, the laser characteristic properties can be predicted to judge the lasing efficiency of the prepared glasses. In the present investigation, the effect of Nd^{3+} ions in different concentrations (0.1, 0.5, 1.0 and 2.0 mol %) modifies the behavior on the intensities of emission bands are reported and the results are compared with certain pertinent glasses reported earlier.

EXPERIMENTAL STUDIES

Synthesis of Nd^{3+} -doped lead borosilicate glasses

High purity chemicals of PbO, H_3BO_3, SiO_2, Al_2O_3, LiF and Nd_2O_3 (99.99) were selected as raw materials for the preparation of Nd^{3+} - doped lead borosilicate (LBS) glasses by the melt-quench procedure. The selected chemical constituents were collected into a clean and dry agate mortar and thoroughly mixed for 30 min. The well mixed batches were taken in a porcelain crucible and kept in a programmable electric furnace and allowed for melting about 1 hr. The molten liquid was poured on the preheated brass mould to obtain transparent glass and also to avoid cracks. The casted glasses are kept for annealing for 10 hours at 400 ^OC and then allowed to cool to room temperature in another furnace to remove the internal stress and strains present in the glasses.

The obtained glasses were polished by using various grades of cerium oxide powders and silicon carbide emery sheets. The molar composition (in mol %) and labeling of the prepared glasses are presented in **Table 1**. The color of the un-doped LBS glass (NLBS0.0) is white, while Nd^{3+} doped LBS glasses are turn into purple color due to the activation of Nd^{3+}ions in the host glass (NLBS0.0). The prepared NLBS glasses were shown in the **Fig.1.**

Table 1. Glass composition and coding of the NLBSX (X= 0.1, 0.5, 1.0 and 2.0 mol%) glasses

Glass composition (mol %)	Code
40 H_3BO_3-**30.0**PbO-10 SiO_2-10 Al_2O_3-10LiF-**0.0 Nd_2O_3**	**NLBS0.0**
40 H_3BO_3-**29.9**PbO-10 SiO_2-10 Al_2O_3-10LiF-**0.1 Nd_2O_3**	**NLBS0.1**
40 H_3BO_3-**29.5**PbO-10 SiO_2-10 Al_2O_3-10LiF-**0.5 Nd_2O_3**	**NLBS0.5**
40 H_3BO_3-**29.0**PbO-10 SiO_2-10 Al_2O_3-10LiF-**1.0 Nd_2O_3**	**NLBS1.0**
40 H_3BO_3-**28.0**PbO-10 SiO_2-10 Al_2O_3-10LiF-**2.0 Nd_2O_3**	**NLBS2.0**

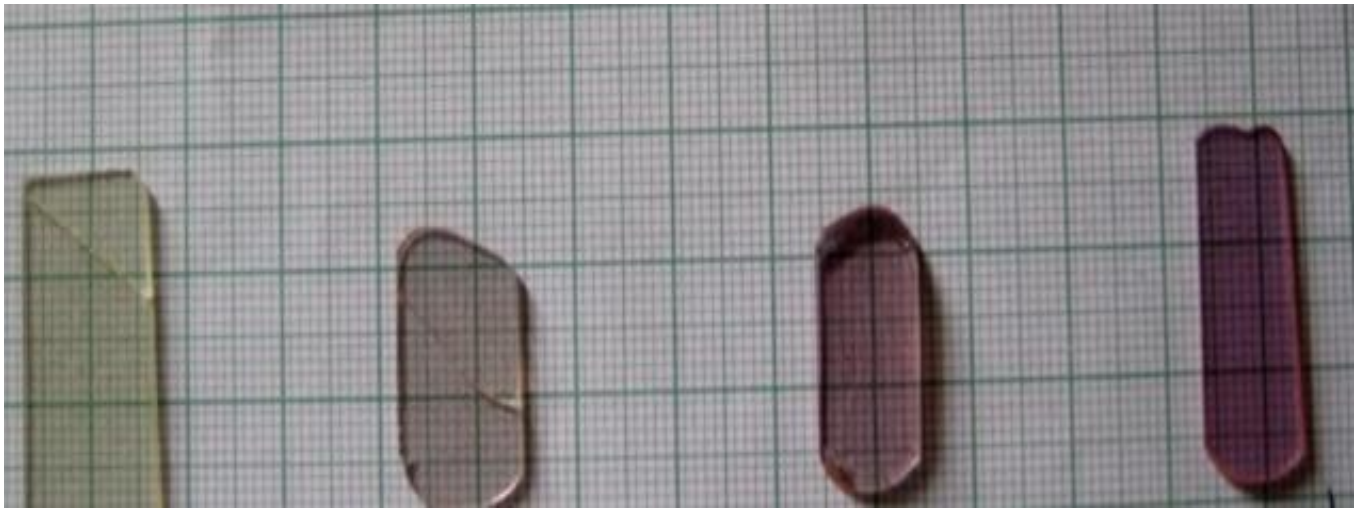

(i) NLBS0.1 **(ii) NLBS0.5** **(iii) NLBS1.0** **(iv) NLBS2.0**

Figure 1. Nd^{3+} doped lead borosilicate glasses

Characterization of Nd^{3+}- doped LBS glasses

The refractive indices of the glasses were found using the Abbe's refractometer using sodium vapour lamp as a light source. The densities of the NLBSX (X = 0.1, 0.5, 1.0 and 2.0 mol %) were determined by the Archimedes method using water as an immersion liquid. The X-ray diffraction pattern was recorded between the angles 10^0 to 80^0 by using Philips X'Pert MPD X-ray diffractometer. The infrared (IR) spectrum was recorded by Perkin-Elmer (PE580) spectrometer in the range of 4000-400 cm^{-1}. Absorption spectrum for NLBS1.0 glass was recorded in the wavelength 400-900 nm using a JASCO V-770 UV-VIS-NIR spectrophotometer with the spectral resolution of 0.1 nm. The photoluminescence spectra as well as the decay profiles were measured using FLS 980 spectrometer.

RESULTS AND DISCUSSION

Physical properties

For the Nd^{3+} - doped LBS glasses, refractive indices (n) and the Nd^{3+} ions concentrations (C) were determined. From these values, the other dependent physical properties such as oxygen packaging density (O), inter-ionic distance (r_i), polaron radius (r_p) and field strength (F) have been calculated by using the expressions given in the literature **[21]** and are presented in **Table 2**. It is observed that, with the increase of Nd^{3+} ions concentration the inter-ionic distance and the polaron radius decreases. It could be due to the increase of the packing fraction of the atoms. The refractive index of a glass depends on number of individual ions exists in the glass and increases with the polarizability of cations.

Table 2. Certain physical properties of NLBSX (X= 0.1, 0.5, 1.0 and 2.0 mol%) glasses

S.No.	Property	NLBS0.0	NLBS0.1	NLBS0.5	NLBS1.0	NLBS2.0
(i)	Refractive index	1.51	1.520	1.54	1.55	1.57
(ii)	Nd^{3+} concentration (n) in 10^{20} ions/cc	0	0.481	2.348	5.252	9.540
(iii)	Oxygen packaging density (O) m^3/mole	6.89	8.024	8.057	8.116	8.178
(iv)	Inter-ionic distance (r_i) A^o	0	26.68	15.71	12.00	9.83
(v)	Polaron radius (r_p) A^o	0	10.74	6.328	4.836	3.962
(vi)	Field strength (F) in 10^{14} cm^{-2}	0	2.60	7.50	12.82	19.11

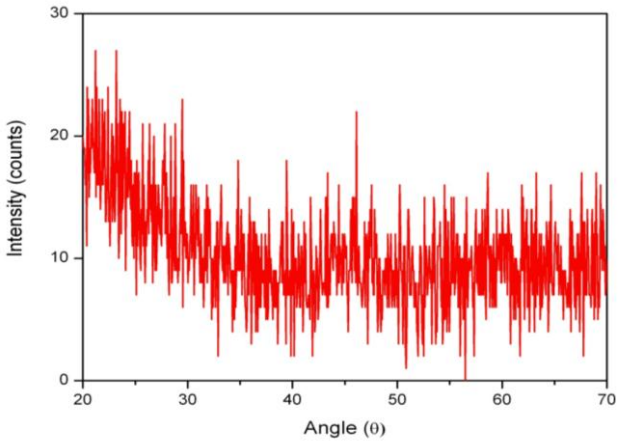

Figure 2. XRD pattern of NLBS0.0 glass (host glass)

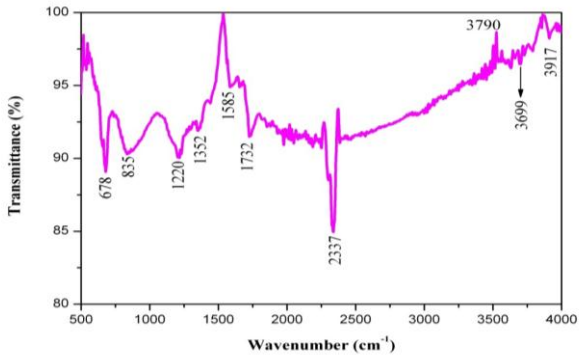

Figure 3. FTIR spectrum of NLBS0.0 glass (host glass)

Structural studies

The XRD pattern of un-doped lead borosilicate host glass shown in **Fig. 2** reveals the absence of sharps peaks in the spectrum which clearly indicates the non-crystalline nature of the glass. The presence of functional groups as well as local structural units are identified from the FTIR spectral measurements recorded in the 400-4000 cm^{-1} for the NLBS0.0 glass is shown in **Fig.3**. The spectral profiles exhibited IR bands at 678, 835, 1220, 1352, 1585, 1732, 2337, 3699 and 3917 cm^{-1} reveals the local structures in the LBS glass. The band at 678 cm^{-1} is attributed due to the combined vibrations of BO_4 and PbO_4 units **[22]**. The broad band observed at 835 cm^{-1} indicates the anti-symmetric stretching mode of Pb-O bonds **[23]**. The band at 1220 cm^{-1} is due to the BO_3 stretching vibrations, whereas the band at 1352 cm^{-1} is due to the stretching vibration of B-O in BO_3 units of meta, pyroborate and orthoborate groups **[24, 25]**. The bands at 1585 and 1732 cm^{-1} are assigned to the bending vibrations of H-O-H bonds. The narrow band at 2337 cm^{-1} is due to the anti-symmetric stretching of adsorbed water molecules. The bands at 3699 cm^{-1} and 3917 cm^{-1} are due to the fundamental stretching vibrations of hydroxyl groups **[26, 27]** and the summary various IR bands are reported in the **Table 3.**

Table 3. Observed IR bands along with their assignments of NLBS0.0 glass (host glass)

Observed IR band position(cm^{-1})	Assignments
678	Combined vibrations of BO_4 and PbO_4 units
835	Anti-symmetric stretching mode of Pb-O bonds
1220	BO_3 stretching vibrations
1352	B-O stretching vibration in BO_3 units
1585	Bending vibrations of H-O-H bonds
1732	Bending vibrations of H-O-H bonds
2357	Anti -symmetric stretching of adsorbed water molecules
3699	O-H stretching vibrations
3917	O-H stretching vibrations

Absorption studies of the Nd^{3+}- doped LBS glasses

Fig. 4 shows the optical absorption spectrum of NLBS1.0 glass recorded in the wavelength region of 400 - 950 nm. Due to the absorption of energy by the ground state ($^4I_{9/2}$) Nd^{3+} ions, they get excited to the various excited levels. From the absorption spectrum, eleven absorption bands at 430, 460, 477, 513, 526, 583, 627, 682, 747, 804 and 875 nm are identified corresponding to the transitions $^4I_{9/2}\rightarrow$ $^2P_{1/2}$, $^4G_{11/2}$, $^2G_{9/2}$, $^4G_{9/2}$, $^4G_{7/2}$, $^4G_{5/2}$, $^2H_{11/2}$, $^4F_{9/2}$, $^4F_{7/2}$, $^4F_{5/2}$ and $^4F_{3/2}$ respectively. The assignments of the transitions have been done based on the reports by the Carnal et.al **[28]**. Among these energy levels, the $^2P_{1/2}$, $^4G_{11/2}$, $^2G_{9/2}$, and $^2H_{11/2}$ levels are not well resolved due to the strong absorption of the host glass. The observed absorption bands in the present work are similar to those of other Nd^{3+} doped glasses, which indicate homogeneous incorporation of the rare earth ions in the glass network. It is also noticed that the bands at 526, 583, 747 and 804 nm are more intense than other bands. In the case of rare earths ions certain transitions are sensitive to ligand environment of the host and these transitions are called as hypersensitive transitions, obeying the selection rules $\Delta J\leq 2$, $\Delta L\geq 2$ and $\Delta S = 0$. These transitions posses higher reduced matrix elements ($\|U^2\|$ and also higher oscillator strengths with respect to other transitions. In the case of Nd^{3+} ion, the $^4I_{9/2}\rightarrow{}^4G_{5/2}$ is the hypersensitive transition and possesses higher oscillator strength.

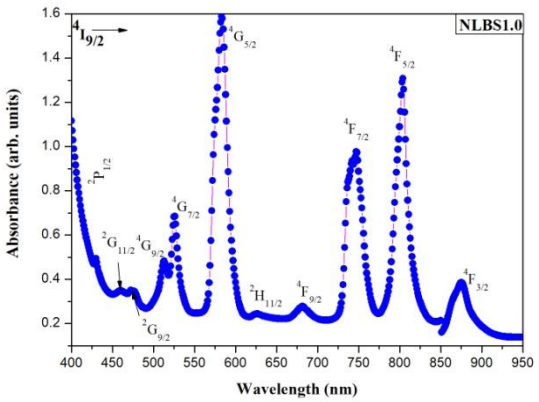

Figure 4. Absorption spectrum of NLBS1.0 glass along with the assignment of absorption bands

Judd-Ofelt analysis

To investigate the nature of bonding that exists between the rare earth ions and the surrounding ligands and as well as the symmetry around the rare earth ions, the JO analysis has been adopted. The JO theory enables the evaluation of intensity parameters Ω_λ (λ = 2, 4 and 6), which are useful to know the nature of the bonding, asymmetry and also in the prediction of certain radiative parameters. To evaluate the JO intensity parameters, the experimental (f_{exp}) oscillator strengths are determined using the expression **[29]**

$$f_{exp} = 4.32\times10^{-9}\int \varepsilon(\nu)\, d\nu \qquad (1)$$

where (ν) is the molar extinction coefficient of the each band at an energy of $\nu(cm^{-1})$

According to the Judd-Ofelt theory, the calculated oscillator strengths (f_{cal}) are given by

$$f_{cal} = \left[\frac{8\pi^2 mc\nu}{3h(2J+1)}\right]\chi \times \sum_{\lambda=2,4,6}\Omega_\lambda \left(\Psi J\left\|U^\lambda\right\|\Psi' J'\right) \qquad (2)$$

where m is the mass of the electron, c is velocity of light, h is Planck's constant, ν is the mean energy of the transition, $\chi = \frac{n(n^2+2)^2}{9}$ is the effective field correction at a well-localized centre in a medium of isotropic refractive index n, Ω_λ (λ = 2, 4 and 6) are called as the Judd-Ofelt intensity parameters and $\left\|U^\lambda\right\|^2$ are the squared reduced matrix elements of the unit tensor operator of the rank λ, which are calculated from the intermediate coupling approximation for a transition $\psi J \rightarrow \psi' J'$.

From the experimental oscillator strengths (f_{exp}) and by using the Judd-Ofelt analysis, the calculated oscillator strengths (f_{cal}) as well as the intensity parameters are obtained by equating the expressions (1) and (2) are presented in **Table 4**.

Table 4. Experimental (f_{exp}) and calculated (f_{cal}) oscillator strengths of NLBS1.0 glass

Transition from $^4I_{9/2}$	Energy (cm^{-1})	Oscillator strengths (10^{-6})	
		f_{exp}	f_{cal}
$^2P_{1/2}$	23,256	0.20	0.21
$^4G_{11/2}$	21,739	0.60	0.49
$^2G_{9/2}$	20,964	0.80	0.83
$^4G_{9/2}$	19,493	2.24	2.23
$^4G_{7/2}$	19,011	4.26	4.15
$^4G_{5/2}$	17,153	25.58	25.59
$^2H_{11/2}$	15,949	0.28	0.49
$^4F_{9/2}$	14,663	1.78	1.82
$^4F_{7/2}$	13,387	10.51	9.43
$^4F_{5/2}$	12,438	13.41	14.10
$^4F_{3/2}$	11,429	1.81	1.24
σ_{rms}		$\pm 0.45\times10^{-6}$	

In our investigation, higher f_{exp} and f_{cal} values are observed for the transition $^4I_{9/2}\rightarrow{}^4G_{5/2}$ which confirms the hypersensitive nature of the transition. The perfectness of the fitting between f_{exp} and f_{cal} has been determined by finding the root mean square deviation (σ_{rms}) using the expression

$$\sigma_{rms} = \left[\frac{\Sigma(f_{exp}-f_{cal})^2}{P}\right]^{1/2} \qquad (3)$$

Here 'P' is the total number of energy levels used in the fitting procedure. In the present work, the observed root mean square deviation (σ_{rms}) *is* 0.45×10^{-6}, which indicates the good fitting between the f_{exp} and f_{cal} values.

Table 5. Comparison of Judd-Ofelt intensity parameters (in 10^{-20} cm^2) of the NLBS1.0 glass with other Nd^{3+} doped host glasses

Glass matrix	Ω_2	Ω_4	Ω_6	Trend	$\chi = \Omega_4/\Omega_6$
NLBS1.0 [Present work]	10.96	1.62	19.87	$\Omega_6>\Omega_2>\Omega_4$	0.081
$30B_2O_3$-70PbO**[30]**	3.52	2.98	5.48	$\Omega_6>\Omega_2>\Omega_4$	0.543
30PbO-$70B_2O_3$ **[30]**	3.96	3.77	4.68	$\Omega_6>\Omega_2>\Omega_4$	0.805
BBO **[31]**	9.95	8.91	12.00	$\Omega_6>\Omega_2>\Omega_4$	0.742
$BINLAB_4$ **[32]**	5.75	5.39	7.69	$\Omega_6>\Omega_2>\Omega_4$	0.700
ZBLAN **[33]**	5.09	3.12	7.16	$\Omega_6>\Omega_2>\Omega_4$	0.435
Silicate[**34]**	4.71	4.54	5.05	$\Omega_6>\Omega_2>\Omega_4$	0.899

The evaluated intensity parameters Ω_λ (λ = 2, 4 and 6) of the NLBS1.0 glass are compared with those of other Nd^{3+} doped glasses as presented in the **Table 5 [30-34]**. The intensity parameter Ω_2 provides the necessary information regarding the nature of symmetry, hypersensitivity and presence of covalence bond between rare earth ion and the ligand environment **[35]**. The parameter Ω_4 mainly depends on the long range effects and related to the bulk properties of the glass, whereas, the Ω_6 parameter provides the information about the rigidity of the host matrix and also electron-phonon coupling strength between the rare earth ion and anion ligands **[36]**.

Photoluminescence studies

Photoluminescence spectra of NLBSX (X=0.1, 0.5, 1.0 and 2.0 mol %) glasses recorded in the region 800-1500 nm with an excitation wavelength of 808 nm are shown in the **Fig 5**. With the given excitation energy, the ground state Nd^{3+} ions are excited to $^4F_{5/2}$ energy level and then return non-radiatively to the $^4F_{3/2}$ metastable state. From the metastable level, the Nd^{3+} ions return to the lower levels $^4I_{9/2}$, $^4I_{11/2}$ and $^4I_{13/2}$ by emitting the radiation. The spectra revealed three emission bands at 903, 1059 and 1334 nm corresponding to the $^4F_{3/2}\rightarrow{}^4I_{9/2}$, $^4I_{11/2}$ and $^4I_{13/2}$ transitions respectively. It is also observed that the emission intensities increases with the increase of Nd^{3+} ions concentration upto 1.0 mol% and then decreases at higher concentrations. It may be due to concentration quenching as well as the energy transfer between the Nd^{3+} ions. Among the emission transitions, the $^4F_{3/2}\rightarrow{}^4I_{11/2}$ transition at 1060 nm is found be more intense than the other transitions

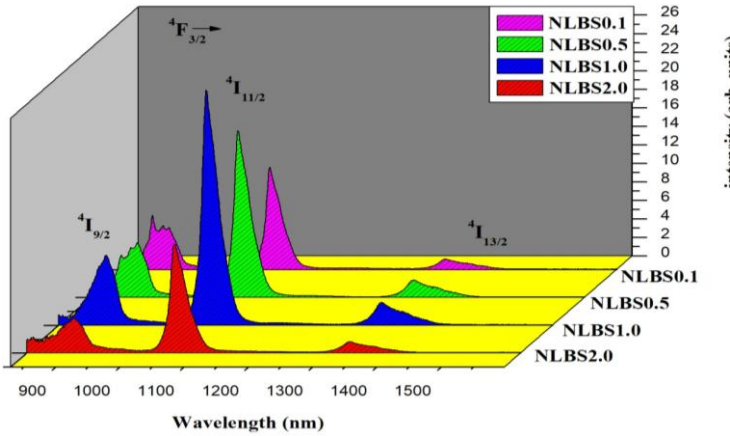

Figure 5. Photoluminescence spectra of NLBSX (X = 0.1, 0.5, 1.0 and 2.0 mol %) glasses

In order to predict the lasing efficiency of Nd^{3+} doped LBS glasses, the evaluated Judd-Ofelt intensity parameters Ω_λ (λ = 2, 4 and 6) are used to calculate the radiative properties such as, spontaneous emission probabilities (A_R), total radiative transition probabilities (A_T), radiative liketimes (τ_R) and branching ratios (β_R) for the $^4F_{3/2}\rightarrow{}^4I_{9/2}$, $^4I_{11/2}$ and $^4I_{13/2}$ emission transitions using the expressions

$$A_{ed} = \frac{64\pi^4\nu^3}{3h(2J+1)}\frac{n(n^2+2)}{9}S_{ed} \quad (4)$$

$$A_{md} = \frac{64\pi^4\nu^3}{3h(2J+1)}n^3 S_{md} \quad (5)$$

The sum of the electric dipole (A_{ed}) and magnetic dipole (A_{md}) transition probabilities gives the radiative transition probability (or) probability for spontaneous emission (A_R) for a transition

$\Psi J \rightarrow \Psi' J'$, as

$$A_R(\Psi J, \Psi J') = A_{ed} + A_{md} \quad (6)$$

$$A_R(\Psi J, \Psi J') = \frac{64\pi^4\nu^3}{3h(2J+1)}\left[\frac{n(n^2+2)^2}{9}S_{ed} + n^3 S_{md}\right] \quad (7)$$

The total radiative transition probability of an excited state is given by the sum of spontaneous emission rates of all the terminal states

$$A_T(\Psi J) = \sum_{\Psi' J'} A_R(\Psi J, \Psi' J') \quad (8)$$

As an excited state ΨJ is relaxed to several lower lying states $\Psi' J'$, the radiative branching ratio

(β_R) is defined as

$$\beta_R(\Psi J, \Psi' J') = \frac{A_R(\Psi J, \Psi' J')}{A_T(\Psi J)} \quad (9)$$

The branching ratios are used to predict the relative intensities of all emission bands originating from a given excited state. The experimental branching ratios (β_{exp}) are determined from the relative areas under the emission bands. The fluorescence branching ratio is a critical parameter for the laser designer, because it characterizes the possibility of attaining stimulated emission for a specific transition. The higher experimental branching ratio will support for the lower threshold value and high gain amplification in lasers. The radiative lifetimes (τ_R) of an excited state (ΨJ) can be extracted from the total radiative transition probability by using the expression

$$\frac{1}{\tau_R} = A_T(\Psi J) = \sum_{\Psi' J'} A_R(\Psi J, \Psi' J') \quad (10)$$

Various calculated radiative parameters are given in **Table 6**. In present work, the higher experimental branching ratios are observed for the $^4F_{3/2} \rightarrow {}^4I_{11/2}$ transition at 1060 nm for all the Nd^{3+}- doped LBS glasses which are useful for high gain broadband amplification applications. According to Jacob and Weber **[37]**, the radiative properties also depend on the ratio of Ω_4/Ω_6, which is called the spectroscopic quality factor (SQF). The SQF helps to identify the efficient channel emission from the $^4F_{3/2}$excited metastable state to the lower levels. For all the prepared glasses, the SQF is < 1, and therefore one can conclude that the $^4F_{3/2} \rightarrow {}^4I_{11/2}$ transition is the most potential transition in the Nd^{3+} doped LBS glasses for laser applications.

Table 6. Different radiative parameters of NLBSX glasses (X= 0.1, 0.5, 1.0 and 2.0 mol%) glasses

Transition	Property	NLBS0.1	NLBS0.5	NLBS1.0	NLBS2.0
$^4F_{3/2} \rightarrow {}^4I_{9/2}$	A_R	1368	5117	4356.1	5942
	A_T	7221	13054	11013	13083
	β_m	0.35	0.26	0.25	0.45
	β_R	0.19	0.39	0.4	0.21
	τ_R(μs)	138	95	82	76
$^4F_{3/2} \rightarrow {}^4I_{11/2}$	A_R	4623	6542	5492	5999
	A_T	7221	13054	11013	13083
	β_m	0.55	0.65	0.66	0.46
	β_R	0.64	0.50	0.50	0.69
	τ_R(μs)	138	95	82	76
$^4F_{3/2} \rightarrow {}^4I_{13/2}$	A_R	1172	1328	1109	1087
	A_T	7221	13054	11013	13083
	β_m	0.1	0.09	0.09	0.1
	β_R	0.16	0.10	0.10	0.10
	τ_R(μs)	138	95	82	76

From the emission spectra of NLBSX (X=0.1, 0.5, 1.0 and 2.0) glasses certain laser characteristic parameters such as stimulated emission cross-sections (σ_e), optical gain bandwidths $(\sigma_e \times \Delta_{eff})$ and optical gain parameters $(\sigma_e \times \tau_R)$are calculated using the expressions

$$\sigma_e = \frac{\lambda_p^4}{8\prod cn^2 \Delta e_{ff}} A_R \quad (11)$$

Optical gain bandwidth = $\sigma_e \times \Delta_{eff}$ (12)

Optical gain =$\sigma_e \times \tau_R$ (13)

and are presented in **Table 7**. From the tabulated data, the NLBS0.5 glass possesses higher values of σ_e, $(\sigma_e \times \Delta_{eff})$ and $(\sigma_e \times \tau_R)$ for the $^4F_{3/2} \rightarrow {}^4I_{11/2}$ transition observed at 1060 nm. The variation of stimulated emission cross-sections of the three emission transitions with Nd^{3+} ions concentration is shown in the **Fig 6**. These results are also compared in **Table 8** with the other Nd^{3+} - doped glasses **[34, 38-39]**. From these studies, it is concluded that the Nd^{3+}- doped LBS glasses are more useful for broadband laser applications.

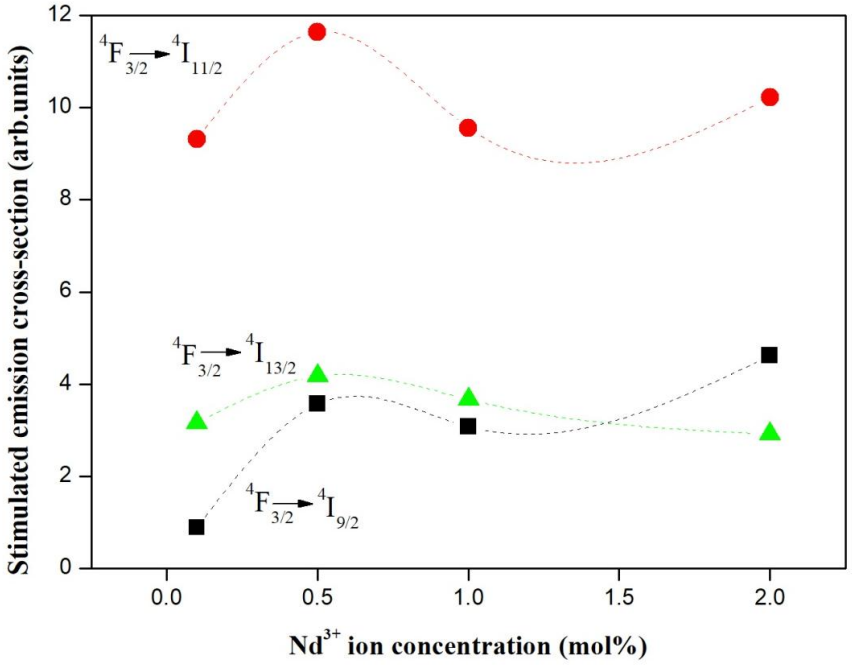

Figure 6. Variation of stimulated emission cross-section of Nd^{3+} - doped LBS glasses for three different emission transitions

Table 7. Laser characteristic parameters such as emission peak positions (λ_P, nm), effective linewidths ($\Delta\lambda_{eff}$, nm), stimulated emission cross-sections (σ_e, $10^{-20}cm^2$), optical gain bandwidths ($(\sigma_e \times \Delta\lambda_{eff})$, $10^{26}cm^3$) and optical gain parameters ($(\sigma_e \times \tau_R)$, $10^{-24}cm^3s^{-1}$), of the NLBSX glasses (X= 0.1, 0.5, 1.0 and 2.0 mol%) glasses

Transition	Lasing parameter	NLBS0.1	NLBS0.5	NLBS1.0	NLBS2.0
$^4F_{3/2} \rightarrow {}^4I_{9/2}$	λ_P	903	902	904	902
	$\Delta\lambda_{eff}$	58.55	53.15	52.26	45.87
	σ_e	0.89	3.57	3.08	4.62
	$\sigma_e \times \Delta\lambda_{eff}$	5.21	18.98	16.09	21.20
	$\sigma_e \times \tau_R$	1.23	3.50	2.53	3.51
$^4F_{3/2} \rightarrow {}^4I_{11/2}$	λ_P	1059	1059	1059	1060
	$\Delta\lambda_P$	35.81	39.54	39.90	39.91
	σ_e	9.32	11.64	9.56	10.22
	$\sigma_e \times \Delta\lambda_{eff}$	33.38	46.02	38.15	40.79
	$\sigma_e \times \tau_R$	12.86	11.05	7.83	7.76
$^4F_{3/2} \rightarrow {}^4I_{13/2}$	λ_P	1334	1334	1337	1334
	$\Delta\lambda_P$	67.53	56.36	53.44	63.57
	σ_e	3.16	4.18	3.67	2.92
	$\sigma_e \times \Delta\lambda_{eff}$	21.35	23.56	19.62	18.57
	$\sigma_e \times \tau_R$	4.36	3.97	3.00	2.21

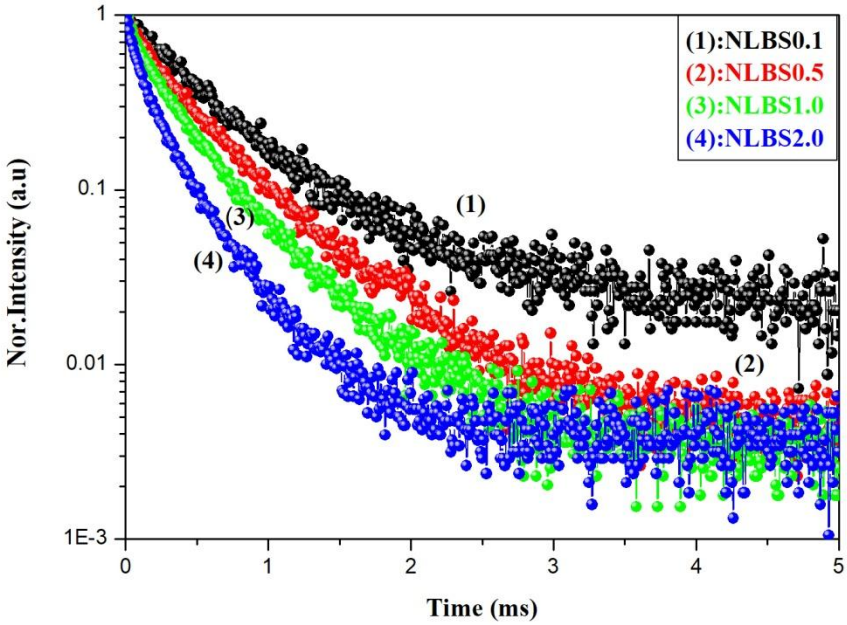

Figure 7. Photoluminescence decay profiles of $^4F_{3/2}$ excited level for different concentrations of Nd^{3+} - doped LBS glasses

Luminescence decay studies

Fig. 7 shows the photoluminescence decay curves for the $^4F_{3/2} \rightarrow {}^4I_{11/2}$ transition at 1060 nm wavelength for different concentrations of Nd^{3+} - doped LBS glasses (0.1, 0.5, 1.0 and 2.0 mol%). From these curves, the experimental lifetimes (τ_{exp}) have been determined using the following expression.

$$\tau = \frac{\int_0^\infty t\, I(t)dt}{\int_0^\infty I(t)dt} \qquad (14)$$

where I(t) is the intensity of the respective decay curve and t I(t) is the multiplication factor of time and intensity. The experimental lifetimes (τ_{exp}) of $^4F_{3/2}$ level are 112, 76, 69 and 62 µs for the 0.1, 0.5, 1.0 and 2.0 mol% concentrations respectively. From these observations, the experimental lifetimes (τ_{exp}) are found to be decrease with the increasing of Nd^{3+} ions concentrations in the LBS glasses. On the other side, the radiative lifetimes (τ_R) obtained from the JO analysis are further used to evaluate the luminescence quantum efficiency (η) of the $^4F_{3/2}$ level from the ratio between the experimental lifetime (τ_{exp}) and the radiative lifetimes (τ_R). The computed quantum efficiencies of $^4F_{3/2}$ level are 81%, 80%, 84% and 81% for the NLBSX glasses (X = 0.1, 0.5, 1.0 and 2.0 mol %) glasses, respectively. It is observed that the higher luminescence quantum efficiency (84%) was found for the NLBS1.0 glass and is suitable for broadband laser applications.

Table 8. Comparison of stimulated emission cross-sections (σ_e , $10^{-20}cm^2$), optical gain bandwidths (($\sigma_e \times \Delta\lambda_{eff}$), $10^{-26}cm^3$) and optical gain parameters (($\sigma_e \times \tau_R$), $10^{-24}cm^3s^{-1}$), for the $^4F_{3/2} \rightarrow {}^4I_{11/2}$ of NLBSX glasses (X= 0.1, 0.5, 1.0 and 2.0 mol%) glasses with other reported glasses

Nd^{3+}doped glass	σ_e	$\sigma_e X\ \Delta\lambda_{eff}$	$\sigma_e X\ \tau_R$	Ref.
NLBS0.1	9.32	33.38	12.86	[Present work]
NLBS0.5	11.64	46.02	11.05	[Present work]
NLBS1.0	9.56	38.15	7.83	[Present work]
NLBS2.0	3.67	40.79	7.76	[Present work]
LTTNd05	1.44	7.59	1.32	**[34]**
LBTAFND05	2.60	8.77	5.98	**[38]**
Flurogallate	2.1	102.9	-	**[39]**

CONCLUSIONS

In the present work, different concentrations of the Nd^{3+} doped LBS glasses were prepared by using the melt-quench method and characterized their structural and spectroscopic properties by using the XRD, FTIR, absorption, photoluminescence and decay spectral measurements. From the XRD analysis, the non-crystalline nature of the prepared LBS glasses has been confirmed and from the FTIR spectrum, various functional groups present in the glass host were identified. From the optical absorption studies, the JO intensity parameters (Ω_λ) were determined from the absorption spectrum of NLBS1.0 glass and their trend has been observed as $\Omega_6 > \Omega_2 > \Omega_4$. The higher Ω_6 parameter of the prepared glass indicates rigidness of the glass and also strong electron-phonon coupling strengths between the Nd^{3+} ions and anion ligands. The radiative properties such as transition

probabilities (A_R), total transition probabilities (A_T), branching ratios (β_R), radiative lifetimes (τ_R) and peak stimulated emission cross sections (σ_e), optical gain bandwidths ($\sigma_e \times \Delta\lambda_{eff}$) and optical gains ($\sigma_e \times \tau_{exp}$) were calculated for all the emission transitions of the Nd^{3+} doped LBS glasses. The higher values of stimulated emission cross sections, optical gain bandwidth and optical gain observed, for the $^4F_{3/2} \rightarrow {}^4I_{11/2}$ transition at 1060 nm suggests that, the present glasses are highly useful for broadband laser applications. From the decay profiles of the $^4F_{3/2} \rightarrow {}^4I_{11/2}$ transition of Nd^{3+} ion, it is concluded that, lifetimes (τ_{exp}) of the $^4F_{3/2}$ level decreased with the increase of Nd^{3+} ion concentrations.

ACKNOWLEDGEMENTS

One of the authors Dr. A. Mohan Babu would like to thank DAE – BRNS, Mumbai, (Letter No.2012/34/72/BRNS) and DST-SERB, New Delhi, (Letter. No. SR/FTP/PS-109/2012) for the sanction of research projects. Also, Mr. M. Reddi Babu is thankful to DAE – BRNS, Mumbai for the financial support in the form of SRF in the above project.

REFERENCES

[1] R.G. Denning, J. Mater. Chem. 11 (2001) 19-28.

[2] S. Bauerecker, T. Toch, H.K. Cammenga, Phys. Chem. Chem. Phys. 100 (1996) 1411-1414.

[3] D. de Ligny, G. Panczer, D. Caurant, D.R. Neuville, Opt. Mater. 30 (2008) 1694 –1698.

[4] N.A. Elalaily, R.M. Mahamed, J. Nucl. Mater. 303 (2002) 44-51.

[5] S. Jayaseelan, N. Satyanarayana, M. Venkateswarlu, J. Mater. Sci. 39 (2004) 1717-1720.

[6] G. Venkateswara Rao, N. Veeraiah, P. Yadagiri Reddy, Opt. Mat. 22 (2003) 295-302.

[7] A. Munoz F., Roger J. Reeves, B. Taheri, Richard C. Powell, Douglas H. Blackburn, David C. Cranmer, J. Chem. Phys. 98 (1993) 6083-6088.

[8] M. Ishii, Y. Kuwano, T. Asai, S. Asaba, M. Kawamura, N. Senguttuvan, T. Hayashi, M. Kobayashi, M. Nikl, S. Hosoya, K. Sakai, T. Adachi, T. Oku, H.M. Shimizu, Nucl. Instr. Meth. A 537 (2005) 282-285.

[9] G.C. Righini, S. Pelli, M. Brenci, M. Ferrari, C. Duverger, M. Montagna, R.Dall'Igna, J. Non- Cryst. Solids 284 (2001) 223-229.

[10] A.F Kemper, B. Moritz, J.K. Freeicks, T.P. Devereaux, New J. Phys. 15 (2013) 023003 - 023018.

[11] D.S. Chemla, J. Shah, Nature 411 (2011) 549-557.

[12] M. Straw, S. Randolph, Laser Phys. Lett. 11 (2014) 035601-035608.

[13] S. Haessler, V. Strelkov, L.B. Elouga-Bom, M. Khokhlova, O. Gobert, J.-F. .Hergott, F. Lepetit, M. Perdrix, T. Ozaki, P. Saliers, New J. Phys.15 (2013) 013051-013063.

[14] D.E. Hinkel, Nucl. Fusion 53 (2013) 104027-104039.

[15] S.M. Kaczmarek, Opt. Mater. 19 (2002) 189-194.

[16] N. Soga, K. Hirao, M. Yoshimoto, J. Appl. Phys. 63 (1988) 4451-4454.

[17] W.F. Krupke, IEEE J. Quantum Electron. 7 (1971) 153-159.

[18] M.J. Weber, J. Non-Cryst. Solids 123 (1990) 208-222.

[19] B. R. Judd, Phys. Rev. 127 (1962) 750-761.

[20] G. S. Ofelt, J. Chem. Phys. 37 (1962) 511-520.

[21] M. Reddi Babu, N. Madhusudhana Rao, A. Mohan Babu, Luminescence, 33 (2018) 71-78.

[22] K.K. Mahato, Anitha Rai, S.B. Rai, Spectrochim. Acta Part A 70 (2008) 577-586.

[23] J. Pisarska, L. Zur, T. Goryczka, W.A. Pisarski, J. Rare Earths 29 (2011) 1157-1160.

[24] B.H. Rudramadevi, S. Buddhudu, Ind. J. Pure and Appl. Phys.46 (2008) 825- 832.

[25] D. Rajesh, Y.C. Ratnakaram, M. Seshadri, A. Balakrishna, T. Sachya Krishna, J. Lumin. 132 (2012) 841-849.

[26] M.V. Vijayakumar, B.C. Jamalaiah, K. Ramagopal, R.R. Reddy, J. Lum. 132 (2012) 86-90.

[27] A. Balakrishna, D. Rajesh, Y.C. Ratnakaram, J. Lum. 132 (2012) 2984-2991.

[28] W.T. Carnall, P.R. Fields, K. Rannak, J. Chem. Phys. 49 (1968) 4424 - 4442.

[29] M. Reddi Babu, N. Madhusudhana Rao, A. Mohan Babu, N. Jaidass C. Krishna Moorthi, L. Rama Moorthy, Optik, 127 (2016) 3121-3126.

[30] M.B. Saisudha, J. Ramakrishna, Phys. Rev. 53 (1996) 6186–6196. [$0B_2O_3$-70PbO]

[31] G.V. Vázquez , G. Muñoz H. , I. Camarillo, C. Falcony , U. Caldiño, A. Lira, Opt. Mat. 46 (2015) 97-103. BBO

[32] M. Vijaya Kumar, A. Suresh Kumar, Opt. Mat. 35 (2012) 12-17. $BINLAB_4$

[33] A. Kedziorski, L. Smentek, J. Alloys Compd. 451 (2008) 686–690. ZBLAN

[34] M. Venkateswarlu, Sk. Mahamuda, K. Swapna, M.V.V.K.S. Prasad, A. Srinivasa Rao, A. Mohan Babu, Suman Shakya, G. Vijaya Prakash, Opt. Mat. 39 (2015) 8-15. [silicate]

[35] S. Hüfner (1978) Optical Spectra of Transparent Rare Earth Compounds, Ac. Press USA.

[36] S. Tanabe, T. Ohyagi, S. Todoroki, T. Hanada, N. Soga, J. Appl. Phys. 73 (1993) 8451- 8455.

[37] R.R. Jacobs, M.J. Weber, IEEE J. Quantum Electron. 12 (1976) 102-111.

[38] B.C. Jamalaiah, T. Suhasini, L. Rama Moorthy, II-Gon Kim, Dong-Sun Yoo, Kiwan Jang, J. Lum. 132 (2012) 1144-1149.

[39] Tianfeng Xue, Liyan, Zhang, Junjiang Hu, Meisong Liao, Lili Hu, Opt. Mat. 47 (2015) 24-29.